Mem. S.A.It. Vol. 83, 632

Memorie della

White dwarf masses in intermediate polars observed by the SUZAKU Satellite

Takayuki Yuasa

Japan Aerospace Exploration Agency (JAXA), Institute of Space and Astronautical Science (ISAS), 3-1-1 Yoshinodai, Chuo, Sagamihara, Kanagawa 252-5210, Japan
e-mail: yuasa@astro.isas.jaxa.jp

Abstract. A method which provides white dwarf (WD) mass estimates based on X-ray spectral analysis is presented. An X-ray spectral model of magnetic accreting WD star is numerically constructed assuming a post-shock cooling flow on top of the magnetic pole of a WD. Broad-band X-ray spectra of intermediate polars (IPs) observed with the *Suzaku* X-ray observatory are fitted with the model, and 17 WD mass estimates were obtained. Typical statistical fitting errors are $0.05 - 0.2\ M_{\odot}$, and the average WD mass and the mean iron abundance of the 17 sources are $0.88 \pm 0.23\ M_{\odot}$ and $0.33 \pm 0.14\ Z_{\odot}$, respectively.

Key words. accretion, accretion disks – novae, cataclysmic variables – X-rays: binaries

1. Introduction

Magnetic accreting white dwarfs (WDs) occupies about 10% of the accreting WD binary, or cataclysmic variable, population. Mass accretion in the magnetic accreting WDs is relatively simple compared to those in non-magnetic systems, channelled by the magnetic field lines near a WD, and has been studied for many years (e.g. Aizu 1973). The accreting gas almost freely falls toward the magnetic pole of the WD, and a stationary shock stands near the surface converting kinematic energy of the gas into thermal energy, i.e. the gas is shock heated. The typical temperature of the shock heated gas reaches higher than 10 keV, and the gas, or plasma, emits hard X-rays via optically thin thermal emissions.

Suzaku , the space X-ray observatory, is capable of observing this X-ray emission, covering the wide energy range of 0.5 – 70 keV. We exploit the satellite to study magnetic accreting WDs in detail, especially concentrating on reproducing their spectra. This work is an update of our previous study published as Yuasa et al. (2010).

2. X-ray spectral model of IPs

Procedures for constructing an emission model of magnetic CVs, i.e. a set of physical assumptions, X-ray emission processes, equation formalism, and numerical calculation technique, were previously studied by many authors (e.g. Wu et al. 1994; Cropper et al. 1998, 1999; Ramsay 2000; Suleimanov et al. 2005). Our previous publication, Yuasa et al. (2010), also followed those procedures, and in this paper, we further improved our model by utilizing a plasma cooling function published by Schure et al. (2009) which allows us to free vary abundance of heavy elements of the plasma in the post shock region (PSR). We reexecuted the

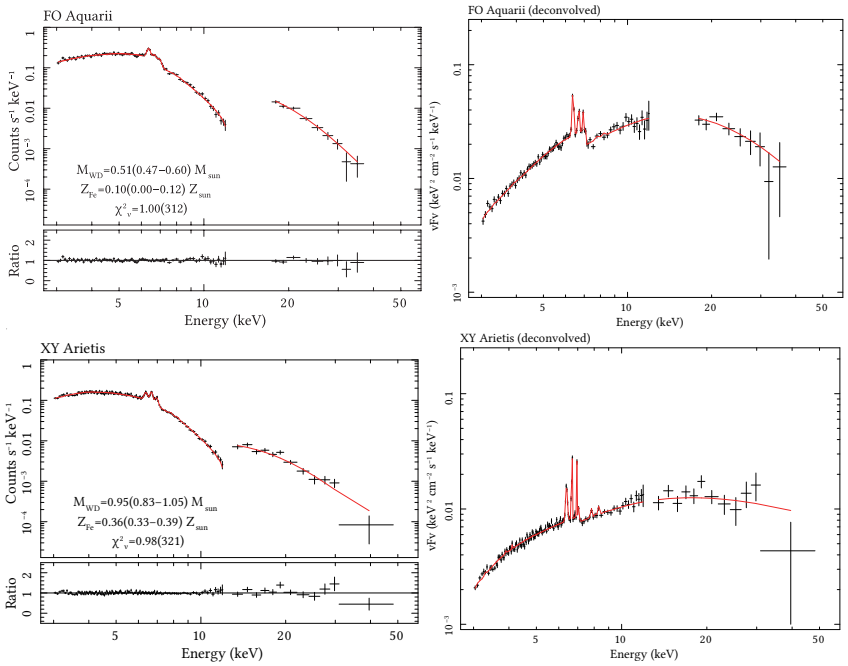

Fig. 1. Observed XIS and HXD spectra (black crosses) of two representative IPs in our sample compared with the best-fit model predictions (solid curves). *Left panels*: Raw spectra, wherein the detector responses are not removed. The lower panels show the data-to-model ratio. *Right panels*: The same spectra, shown after removing the detector responses and multiplied by E^2, or equivalent to the νF_ν representation.

same code described in (Yuasa et al. 2010) with the updated cooling function, and constructed a spectral model called `IP_PSR` which can be loaded to the Xspec spectral analysis package.

3. Spectral fitting

We analyzed spectra of 17 IPs observed with *Suzaku* . This sample covers ∼ 80 % of the X-ray flux limited IPs observed by *Swift* (Brunschweiger et al. 2009), and therefore, can be thought to be a subset of the flux limited sample. When fitting their spectra, we utilized the energy ranges of 3 – 12 and 12 – 50 keV for the X-ray Imaging Spectrometer (XIS) and the Hard X-ray Detector (HXD) onboard *Suzaku* . Notable spectral features of IPs such as the intense Fe emission lines and the thermal spectral cutoff appear in the 6 – 7 keV and > 10 keV bands, and therefore, these energy coverages

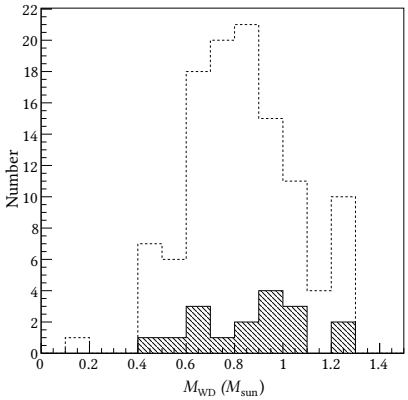

Fig. 2. The WD mass spectrum of our sample IPs (shaded histogram), compared with that of 104 CVs (histogram with dashed line; taken from Ritter & Kolb 2003), derived from optical/infrared spectroscopies.

Table 1. The best-fit spectral parameters obtained with the partial-covering absorber model. The errors are at 90% confidence levels.

System	$Z_{\rm Fe}$ ($Z_\odot$)	$M_{\rm WD}$ ($M_\odot$)	$\chi^2_\nu(\nu)$	System	$Z_{\rm Fe}$ ($Z_\odot$)	$M_{\rm WD}$ ($M_\odot$)	$\chi^2_\nu(\nu)$
FO Aqr	$0.10^{+0.02}_{-0.10}$	$0.51^{+0.09}_{-0.04}$	1.00(312)	EX Hya	$0.55^{+0.04}_{-0.03}$	$0.43^{+0.02}_{-0.02}$	1.31(316)
XY Ari	$0.36^{+0.03}_{-0.03}$	$0.95^{+0.10}_{-0.12}$	0.98(321)	NY Lup	$0.42^{+0.03}_{-0.02}$	$1.26^{+0.04}_{-0.03}$	1.16(251)
MU Cam	$0.49^{+0.07}_{-0.06}$	$0.95^{+0.21}_{-0.22}$	1.12(318)	V2400 Oph	$0.25^{+0.03}_{-0.03}$	$0.66^{+0.05}_{-0.06}$	0.92(319)
BG CMi	$0.18^{+0.04}_{-0.03}$	$1.04^{+0.12}_{-0.10}$	1.13(318)	AO Psc	$0.46^{+0.08}_{-0.04}$	$0.63^{+0.07}_{-0.03}$	1.18(317)
V709 Cas	$0.16^{+0.04}_{-0.03}$	$1.07^{+0.10}_{-0.15}$	1.05(321)	V1223 Sgr	$0.27^{+0.01}_{-0.02}$	$0.79^{+0.04}_{-0.04}$	1.12(252)
TV Col	$0.41^{+0.04}_{-0.03}$	$0.91^{+0.09}_{-0.08}$	1.11(321)	RX J2133	$0.30^{+0.04}_{-0.03}$	$0.83^{+0.13}_{-0.10}$	1.22(194)
TX Col	$0.41^{+0.09}_{-0.09}$	$0.80^{+0.27}_{-0.15}$	1.23(186)	IGR J17303	$0.23^{+0.04}_{-0.04}$	$1.24^{+0.06}_{-0.39}$	1.19(320)
YY Dra	$0.59^{+0.07}_{-0.06}$	$0.93^{+0.15}_{-0.15}$	0.98(318)	IGR J17195	$0.32^{+0.04}_{-0.04}$	$0.94^{+0.11}_{-0.15}$	0.95(321)
PQ Gem	$0.17^{+0.04}_{-0.03}$	$1.09^{+0.09}_{-0.13}$	1.14(303)				

will allow us to precisely catch differences of physical parameters of individual systems, particularly their WD masses.

3.1. Spectral fit model

To take into account the effects of intrinsic absorption caused by accreting matter (Suleimanov et al. 2005), we introduced a concept of partially-covering (PC) photo absorption. This assumes that some fraction of the incident emission (i.e. X-rays from the PSR) suffers from an absorption with a hydrogen column density of $n_{\rm H,PC}$, and the remaining will directly reach us. This is an approximation to the time-variable absorption and the non uniformity of the gas density in the accretion stream itself. The total model thus becomes,

$$\begin{aligned}&\texttt{Total Model}(\text{photons s}^{-1}\text{ cm}^{-2}) \\ &\times[\texttt{Interstellar Ph. Abs.}\ (n_{\rm H})] \\ &\times(C_{\rm PC}\cdot[\texttt{Ph. Abs.}\ (n_{\rm H,PC})]\cdot\texttt{IP\_PSR} \\ &+(1-C_{\rm PC})\cdot\texttt{IP\_PSR}+\texttt{Gaussian} \\ &+\texttt{Gaussian}).\end{aligned} \quad (1)$$

The terms with $C_{\rm PC}$ and $(1-C_{\rm PC})$ represent the absorbed and non-absorbed components, respectively. These two IP_PSR components share the same parameters ($M_{\rm WD}$, $Z_{\rm Fe}$, and normalization). The two Gaussians are for the Kα and Kβ emission lines from neutral irons.

3.2. WD masses estimated from wide-band spectral fitting

Figures 1 shows the spectra and the best-fit models of individual IPs. As evidenced by the best-fit parameters listed in Table 1, the model successfully reproduced the observed spectra in most cases. Looking at the spectra, for example those presented in Figure 1, it can be recognized that the HXD spectrum of FO Aqr is more strongly curved than that of XY Ari. This feature indicates that FO Aqr has a lower PSR shock temperature and hence lower WD mass than XY Ari; derived masses, $0.51^{+0.09}_{-0.04}\ M_\odot$ and $0.95^{+0.10}_{-0.12}\ M_\odot$ for FO Aqr and XY Ari, respectively, are consistent with this apparent properties.

The derived masses are in the range of $0.4-1.3\ M_\odot$ which is consistent with current understanding on the WD mass and its upper limit of $\sim 1.4\ M_\odot$. The average WD mass of $0.88\pm0.23\ M_\odot$ and the mean iron abundance $0.33\pm0.14\ Z_\odot$ were obtained from the present sample including 17 IPs (associated errors are 1σ standard deviations for the distributions).

4. Discussion

4.1. WD mass spectrum and its average

Figure 2 shows the distribution of the WD masses we derived, compared with those of CVs determined kinematically, mainly based on optical/infrared spectroscopy (Ritter & Kolb 2003). The mean mass is obtained

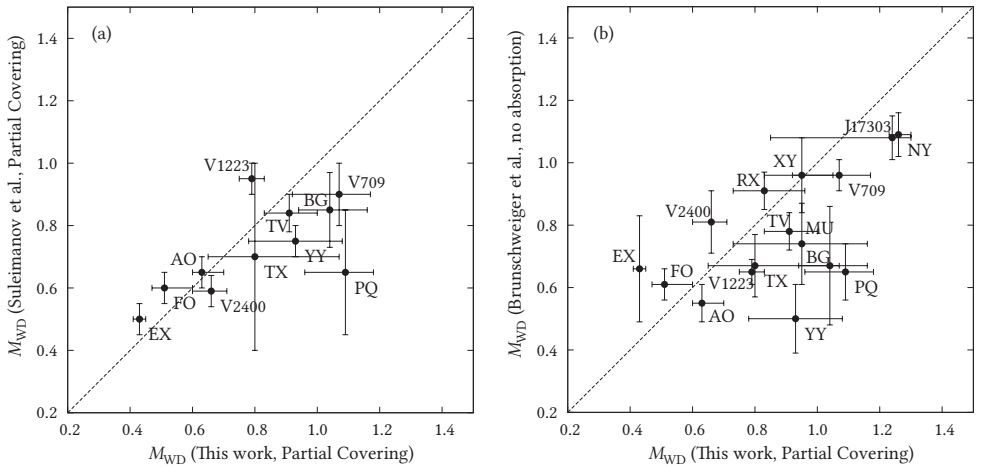

Fig. 3. Comparison of the WD masses estimated in the present study with those by (a) Suleimanov et al. (2005) and (b) Brunschweiger et al. (2009).

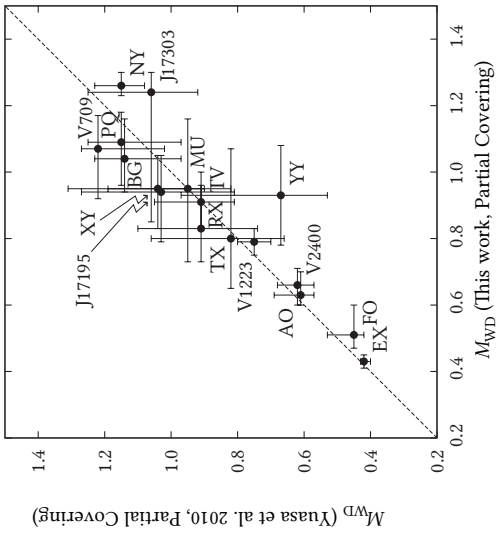

Fig. 4. Comparison of the WD masses estimated in the present study with those by Yuasa et al. (2010).

as 0.88 ± 0.23 $M_\odot$ from the present study and 0.82 ± 0.24 $M_\odot$ from the optical sample (errors are 1σ standard deviations), with a Kolmogorov-Smirnov probability of 0.39. Therefore it is inferred for this limited sample that the mass spectra of CVs and IPs are statistically not largely different.

The mean WD mass of our IP sample, 0.88±0.23 $M_\odot$, can be compared with the value of $\sim 0.5\ M_\odot$ inferred by Krivonos et al. (2007) based on the analysis of Galactic Ridge X-ray Emission (GRXE) in the hard X-ray band with *INTEGRAL*/SPI. Although we are aware that their value ($\sim 0.5\ M_\odot$) was derived from tentative fitting of the GRXE spectrum with an IP model, this comparison is intriguing because IPs are thought to have deep connection with the origin of the GRXE (especially in the hard X-ray band).

4.2. Comparison of the estimated WD masses

In Figure 3, we plot correlations between our WD masses and those from the *RXTE*/PCA+HEXTE data by Suleimanov et al. (2005) and the *Swift*/BAT data by Brunschweiger et al. (2009); the spectral models and the energy band used in these three studies are very similar to one another.

In Figures 3 (a) and (b), our results derive higher WD masses, especially for massive ($\gtrsim 1\ M_\odot$) systems, although rough correlations are seen among the three measurements. For a few sources, for example V709 Cas, BG CMi, and PQ Gem, this discrepancy amounts to $\sim 0.3 - 0.4\ M_\odot$. Reasons for these differ-

ences are unclear at present. Unfortunately, the WD masses of Suleimanov et al. (2005) and Brunschweiger et al. (2009) show the same level of disagreement as seen in these figures, even though the two studies use the same spectral model calculated in the former.

The difference within the same model might indicate that the results suffer from rather large systematic uncertainties of different instruments (*RXTE* /PCA and *Swift* /BAT), which could exceed the quoted statistical fitting errors. We are aware that our analysis is not free, either from possible systematic uncertainties involved in our instruments (*Suzaku* /XIS+HXD) and the spectral model (e.g. accretion rate dependence of the model and an assumption of zero base temperature). Yet we think that our result may be less subject to various systematic effects, because we jointly utilized the Fe-K line spectroscopy and the hard-band continuum shape.

In Yuasa et al. (2010), we have already reported WD mass estimates based on the same *Suzaku* data but with slightly different spectral model. In that paper, a plasma cooling function of Sutherland & Dopita (1993) was used when solving PSR equations, and hence the Fe abundance had to be fixed at 1. In contrast, the present model utilizes an update cooling function of Schure et al. (2009) which also allows variable Fe abundance. As shown in Figure 4, the two results agree well within statistical fitting errors, and thus, it is clear that the WD masses estimated in the present method do not depend on the choice among the currently used cooling functions. Note, however, that the presently updated modeling has higher self-consistency compared to that of Yuasa et al. (2010).

From X-ray light curve analysis in the eclipsing IP XY Ari, Hellier (1997) estimated $M_{\rm WD}$ to be $0.91 - 1.17\ M_{\odot}$. Our result, $M_{\rm WD} = 0.95^{+0.10}_{-0.12}\ M_{\odot}$, nicely agrees with this value, and this agreement provides a convincing calibration to the present methodology (see also Brunschweiger et al. 2009 for a similar argument).

5. Summary

By numerically solving the hydrostatic equations for post-shock regions on top of magnetic CVs (e.g. Suleimanov et al. 2005), we constructed the X-ray spectral model with improvements in terms of a plasma cooling function with variable heavy metal abundance. We fitted spectra of 17 IPs observed with *Suzaku*, and successfully reproduced the Fe line structures in the $6 - 7$ keV band and at the same time the thermal cutoff detected in the hard X-ray band. From the best-fit models, we estimated the WD masses and the Fe abundances. The average WD mass for the present sample were $0.88 \pm 0.23\ M_{\odot}$. All sources exhibited sub-solar Fe abundance, with the average being $0.33 \pm 0.14\ Z_{\odot}$. The WD mass of the newly found IP, IGR J17195-4100, was estimated to be $0.94^{+0.11}_{-0.15}\ M_{\odot}$.

References

Aizu, K. 1973, Progress of Theoretical Physics, 49, 1184
Brunschweiger, J., Greiner, J., Ajello, M., & Osborne, J. 2009, A&A, 496, 121
Cropper, M., Ramsay, G., & Wu, K. 1998, MNRAS, 293, 222
Cropper, M., Wu, K., Ramsay, G., & Kocabiyik, A. 1999, MNRAS, 306, 684
Hellier, C. 1997, MNRAS, 291, 71
Krivonos, R., , et al. 2007, A&A, 463, 957
Ramsay, G. 2000, MNRAS, 314, 403
Ritter, H. & Kolb, U. 2003, A&A, 404, 301
Schure, K.M., et al. 2009, A&A, 508, 751
Suleimanov, V., Revnivtsev, M., & Ritter, H. 2005, A&A, 435, 191
Sutherland, R.?S. & Dopita, M. A. 1993, ApJS, 88, 253
Wu, K., Chanmugam, G., & Shaviv, G. 1994, ApJ, 426, 664
Yuasa, T., et al. 2010, A&A, 520, A25